

# Gamma Ray Bursts

Peter Mészáros

Center for Particle and Gravitational Astrophysics  
Dept. of Astronomy & Astrophysics and Dept. of Physics  
Pennsylvania State University, University Park, PA 16802, USA

## Abstract

Gamma-ray bursts have been detected at photon energies up to tens of GeV. We review some recent developments in the X-ray to GeV photon phenomenology in the light of *Swift* and *Fermi* observations, and some of the theoretical models developed to explain them, with a view towards implications for C.T.A.

## 1 Introduction

Gamma-ray bursts (GRB) are brief events occurring at an average rate of a few per day throughout the universe, which for a period of seconds flood with their radiation an otherwise almost dark gamma-ray sky. While they are on, they far outshine all other sources of gamma-rays in the sky, including the Sun. In fact, they are the most concentrated and brightest electromagnetic explosions in the Universe. Since the discovery in 1997 by the *Beppo-SAX* satellite of GRB X-ray afterglows, which enabled ground-based telescopes to detect their optical counterparts, we know that these objects are at cosmological distances. Thanks mainly to the subsequent *Swift* satellite, we now have detailed multi-wavelength data for many hundreds of bursts, and redshifts for over 150. In fact, the GRB prompt electromagnetic energy output during tens of seconds is comparable to that of the Sun over  $\sim \text{few} \times 10^{10}$  years, or to that of our entire Milky Way over a few years; and their X-ray afterglow over the first day after the outburst can outshine the brightest X-ray quasars.

The current interpretation of this spectacular phenomenon is that about a solar rest mass worth of gravitational energy is released in a very short time (seconds or less) in a small region of the order of tens of kilometers by a cataclysmic stellar event. The latter, in some cases, is the collapse of the core of a massive star, or in some cases may be the merger of two compact stellar remnants, ultimately leading to a black hole. The mainstream GRB scenario envisions that only a small fraction of this energy is converted into electromagnetic radiation, through the dissipation of the kinetic energy of

a collimated relativistic outflow, a “fireball” with bulk Lorentz factors of  $\Gamma \gtrsim 300$ , expanding out from the central engine powered by the gravitational accretion of surrounding matter into the collapsed core or black hole.

The most often invoked mechanisms for generating the observed non-thermal photons are synchrotron radiation and/or inverse Compton (IC) scattering by relativistic electrons which have been accelerated to a power-law distribution in the shocks expected in the optically thin regions of the outflow. These may be internal shocks, resulting in prompt  $\gamma$ -ray emission, and also external shocks at the termination of the relativistic outflow, which can explain many of the properties of the afterglows. Other mechanisms considered for the prompt emission are, e.g., magnetic dissipation or reconnection in the outflow, jitter radiation in shocks, or dissipative effects in the photosphere where the outflow transitions to optical thinness.

More recently the *LAT* instrument onboard the *Fermi* spacecraft, extending previous preliminary observations by *EGRET* on the Compton *CGRO* satellite, has shown that a substantial fraction of GRBs have photon spectra which extend at least to tens of GeV [6, 3, 8]. These could be due either to leptonic mechanisms such as mentioned above, or perhaps could be related to hadronic effects. The uncertainty about the mechanism is, in part, due to lack of knowledge about two important parameters of the outflow. These are the baryon load of the outflow, and the magnetic ratio  $\sigma$  between magnetic stresses and kinetic energy, which affect not only the bulk dynamics but also the possibility of accelerating protons in the shocks or the dissipation region. Accelerated protons could lead in principle to GRBs being as (or perhaps more) luminous in cosmic rays and neutrinos than in the commonly observed sub-MeV electromagnetic channels, in addition to predicting significant secondary GeV and TeV photon fluxes.

## 2 GRB Phenomenology: MeV to Multi-GeV

Soon after its launch in late 2008, *Fermi* started detecting GRBs with both its instruments, the Large Area Telescope (*LAT*, 20 MeV to  $> 300$  GeV) and the Gamma-ray Burst Monitor (*GBM*, 8 keV to 40 MeV), which together cover more than seven decades in energy. While in its first 2.5 years the *GBM* has triggered on bursts at a rate of about  $250 \text{ yr}^{-1}$ , of which on average  $\sim 205$  are long bursts and  $\sim 45$  are short bursts, the *LAT* detected  $\sim 25$  bursts in the same period at  $\geq 100$  MeV, i.e.  $\sim 9 \text{ yr}^{-1}$ ; or, in the same

period at  $\geq 1$  GeV it detected  $\sim 12$ , i.e.  $\sim 5 \text{ yr}^{-1}$

The brightest *LAT* bursts as of September 2011, GRB 080916C [15], GRB 090510 [16, 12], GRB 090902B [17], and GRB 090926A [18], have yielded hundreds of  $\gtrsim 100$  MeV photons each, and together with the lower energy *GBM* observations have yielded unprecedented broad-band spectra. An interesting and unexpected behavior is that in many cases the GeV emission starts with a noticeable delay after the MeV emission. E.g. in GRB 080916C, the GeV emission appears only in a second pulse, delayed by  $\sim 4$  s relative to the first pulse (visible only in MeV); see Fig. 1. Such a delay is present also in short bursts, such as GRB 090510, where it is a fraction of a second. This soft-to-hard spectral evolution is clearly seen in all five of the bright *LAT* bursts above, and to various degrees a similar behavior is seen in other weaker *LAT* bursts.

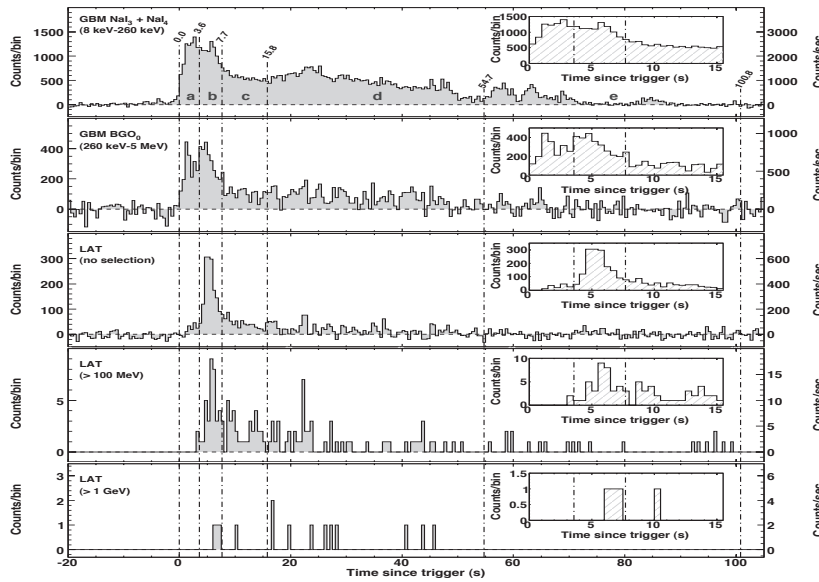


Figure 1:  
Light  
curves of  
GRB080916C  
with the  
*GBM* (top  
two curves)  
and  
*LAT* (bot-  
tom three  
curves)[15].

In some burst, such as GRB 080916C and several others, the broad-band gamma-ray spectra consisted of simple Band-type broken power law function in *all* time bins (similar to spectrum in time bin [a] of Fig. 2). In GRB 080916C the first pulse had a soft high energy index disappearing at GeV, while the second and subsequent pulses had harder high energy indices reaching into the multi-GeV range. The absence of statistically significant evidence for a distinct high energy spectral component in a number of the earlier *LAT* bursts was puzzling, since such an extra component is naively

expected from inverse Compton or hadronic effects. Instead, in each time bin a single broken power spectrum straddled the *GBM* and (except for the earliest times) the *LAT* ranges. The peak energy of the Band function evolved from soft to hard and back to soft, and in GRB 080916C as well as in other *LAT* bursts, the GeV emission persisted into the afterglow phase, typically lasting  $\gtrsim 500 - 1000$  s.

On the other hand, in some bursts, such as GRB090510 [16, 12] and GRB 090902B [17], a second hard spectral component extending above 10 GeV without any obvious break appears in addition to common Band spectral component dominant in the lower 8 keV-10 MeV band. A similar second hard component is also present in GRB 090926A (Fig. 2), where in one time bin it shows a turnover around a few GeV. Such a second component, if present in GRB 080916C and GRB 110731A, was not significant enough to claim detection.

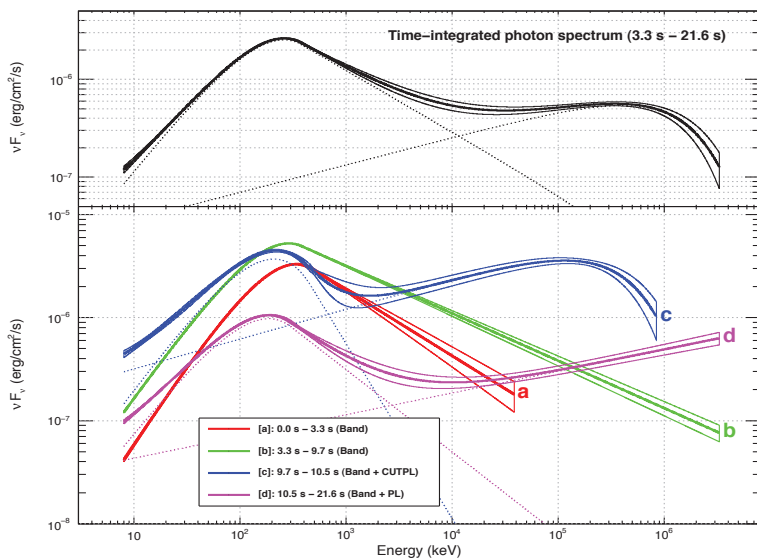


Figure 2: Spectra of GRB090926A from *Fermi* at four different time intervals, a= [0.0-3.3s], b= [3.3-9.7s], c= [9.7-10.5s], d= [10.5-21.6s] [18].

Furthermore, in some bursts such as GRB 090510 and GRB 090902B, the same 2nd power-law component that dominates above  $\sim 100$  MeV also extends below the Band component, and dominates below  $\sim 50$  keV. This low energy power law extension (i.e. flatter and lying below the Band component) is also detected in at least two other bright GBM short bursts, GRB 090227B and GRB 090228, which have not been detected by the *LAT* [19].

An exciting discovery, unanticipated by *EGRET*, was the detection of

high-energy emission from two short bursts (GRB 081024B [11] and GRB 090510 [12]), whose general behavior (including a GeV delay) is qualitatively similar to that of long bursts. The ratio of short to long GRBs is  $\sim 10 - 20\%$ , both for objects detected at  $\geq 100$  MeV and for those detected only at  $\lesssim 1$  MeV. However, while the statistics on short GRBs are too small to draw firm conclusions, so far, the ratio of the *LAT* fluence to the *GBM* fluence is  $> 100\%$  for the short bursts as compared to  $\sim 5 - 60\%$  for the long bursts. Thus, although fewer in number, if the acquisition is fast enough CTA might be able to detect short bursts.

It is also noteworthy that, for both long and short GRBs, the  $\geq 100$  MeV emission lasts longer than the *GBM* emission in the  $\lesssim 1$  MeV range. The flux of the long-lived *LAT* emission decays as a power law with time, which is more reminiscent of the smooth temporal decay of the afterglow X-ray and optical fluxes rather than the variable temporal structure in the prompt keV–MeV flux. This similarity in the smooth temporal evolution of the fluxes in different wave bands has been detected most clearly from GRB 090510 [13, 14], although this object also requires a separate prompt component to the *LAT* emission [21]. This short burst was at  $z = 0.9$ , and was jointly observed by the *Fermi LAT*, *GBM* and by the *Swift* Burst Alert Telescope (BAT), the X-Ray Telescope (XRT), and the UV and Optical Telescope (UVOT). The longest-lived emission detected by the *Fermi LAT* is  $\sim 130$  minutes, from GRB 090328, longer than the EGRET observation of GRB 940217 [9] without any earth occultation.

Interestingly, the *LAT* detected only  $\lesssim 10\%$  of the bursts triggered by the *GBM* which were in the common *GBM* -*LAT* field of view. This may be related to the fact that the *LAT*-detected GRBs, both long and short, are generally among the highest fluence bursts, as well as being among the intrinsically most energetic GRBs. For instance, GRB 080916C was at  $z = 4.35$  and had an isotropic-equivalent energy of  $E_{\gamma,\text{iso}} \approx 8.8 \times 10^{54}$  ergs in  $\gamma$  rays, the largest ever measured from any burst [15]. The long *LAT* bursts GRB 090902B [17] at  $z = 1.82$  had  $E_{\gamma,\text{iso}} \approx 3.6 \times 10^{54}$  ergs, while GRB 090926A [18] at  $z = 2.10$  had  $E_{\gamma,\text{iso}} \approx 2.24 \times 10^{54}$  ergs. Even the short burst GRB 090510 at  $z = 0.903$  produced, within the first 2 s, an  $E_{\gamma,\text{iso}} \approx 1.1 \times 10^{53}$  ergs [12].

### 3 Simple Leptonic Models

The standard internal and external shock models are the ones most commonly used in interpreting the *Fermi* data on GRBs, as was previously the case with *Swift* data. In the latter, the amount and quality of data was so large and detailed that various extensions and refinements to the simpler standard model were considered, and the need for this is becoming apparent also for *Fermi* analyses, even though, particularly for the *LAT*, the statistics are only gradually building up.

Most of these models are leptonic, e.g. internal plus external forward shock models were proposed for individual bursts, e.g. [13, 10], etc. Broader formulations have attempted to cover *LAT* bursts in general, e.g. [26], based on the first three *LAT* bursts, argued that the GeV extended emission decays roughly as  $F \propto t^{-1.5}$ , with *LAT* spectra of approximate form  $F_E \propto E^{-1}$  which did not evolve strongly. This, they proposed, can be due to a *radiative* (fast cooling) forward shock, where the Lorentz factor evolves as  $\Gamma \propto t^{-3/7}$  and the luminosity as  $L \propto T^{-10/7}$ . To satisfy the fast cooling ( $t_{cool} \leq t_{dyn}$ ) condition in the long-lasting afterglow phase, they proposed that high energy photons back-scattered towards the source would provide copious  $e^\pm$  pairs, enhancing the cooling. Without going into details, they argued that the external shock (GeV) emission would naturally start later than the prompt MeV emission (e.g. from internal shocks or similar origin; see also [118]).

Alternatively, assuming different power laws through the error bars of the same burst data, an *adiabatic* forward shock may also provide a fit [87, 89]. In this scenario the rough similarity of the spectra and decay slopes in several bursts might be due to the GeV emission being above the characteristic synchrotron cooling and peak energies  $E_c$ ,  $E_m$ , where the behavior is insensitive to the initial  $\Gamma$  and to the external density  $n$ , leading to a decay  $F \propto t^{-1.2}$  typical of adiabatic forward shocks. These authors obtain a range of external densities for which the external shock emission is not dominated by the high energy extension of the prompt. Interestingly, these include solutions where the pre-shock magnetic field need not be much greater than interstellar fields,  $B_{ext} \gtrsim 10 \mu\text{G}$ , to yield after shock compression a synchrotron flux comparable to that observed, provided the external densities are uncommonly low,  $n_{ext} \lesssim 10^{-5} \text{ cm}^{-3}$ , which may be difficult (c.f. also [43, 27]).

The inclusion of more detailed physics can explain some of the departures from the simplest forward shock models seen in the data. For instance [91] show that Klein-Nishina (KN) effects on the SSC upscattering can alter the

synchrotron source photon flux in a time-dependent manner. The scattering  $Y$ -parameter is initially low at GeV energies due to KN effects, and weak at X-ray energies, leading to strong GeV synchrotron and weak X-ray/optical emission. Later the KN effect weakens,  $Y$  increases and the GeV synchrotron light curve decays more steeply than the  $t^{-1.2}$  of simple adiabatic shocks. Inclusion of these effects also shows [21] that in GRB 090510 the GeV emission in the first 4-5 s must have an origin other than the simple forward shock, probably being related to the prompt emission.

The bulk Lorentz factors  $\Gamma$  obtained from  $\gamma\gamma$  pair production opacity arguments in the prompt emission of bright *LAT* GRB models such as the above turned out to be larger than previously expected,  $500 \lesssim \Gamma \lesssim 10^3$ ) [15, 12, 17, 18]. These constraints were based on simple one-zone models, however, and the value depends on model details (e.g. [4, 23]), which are vague at present. Nonetheless, fairly general arguments lead to the conclusion [28] that for the large luminosities  $L_{\gamma,\text{iso}} \gtrsim 10^{54}$  erg s $^{-1}$  inferred in *LAT* GRBs, photons of energy  $E_\gamma \gtrsim 10$  GeV cannot emerge from radii much smaller than  $r_{\gamma\gamma} \sim 10^{15}$  cm (e.g. [24]). The two highest-energy (observer frame) photons of 13.2 GeV and 33.4 GeV, detected from GRB 080916C at  $z = 4.35$  and GRB 090902B at  $z = 1.82$ , provide through  $\gamma\gamma$  pair production opacity arguments the best constraints so far [25] on models of Extragalactic Background Light (EBL) predicting a high optical-UV intensity.

Perhaps the most exciting, or exotic, consequence of the observed delays between the *LAT* GeV emission and the *GBM* MeV emission is that it can be used to set robust constraints on effective field theory formulations of quantum gravity. In particular it rules out a first order dependence on  $(E_\gamma/E_{\text{Planck}})$  of any Lorentz invariance violating (LIV) terms, using GRB 090510 data [16].

## 4 More Detailed Leptonic Models

Attempts at explaining the observed GeV-MeV time delays in the context of simple one-zone leptonic Synchrotron-Self-Compton (SSC) mechanisms generally encounter difficulties, e.g. [12, 30]. This is the main observational motivation for considering two- or multiple zone models, typically involving an inner softer source whose photons are up-scattered by electrons in a different region further out. One example [31] invokes upscattering of X-ray

photons from the GRB jet’s waste-heat cocoon by internal shock electrons. The delayed photons arise from the high latitude brighter emission and since the cocoon Lorentz factor is much smaller than that of the jet, the emission time from the cocoon is delayed relative to that of the jet internal shock emission. This results in two spectral components, but in some parameter ranges it can also mimic a single Band component.

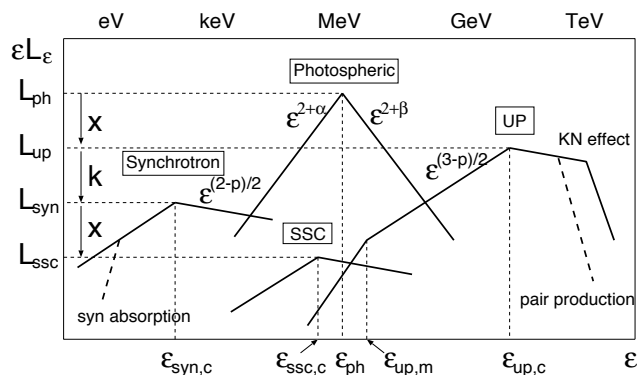


Figure 3: Schematic broadband spectrum for a leptonic photospheric-internal shock model of the MeV to GeV emission of GRB (see text) [32].

Another source of soft photons may be the jet scattering photosphere, which in some models is thought to be responsible for the Band (MeV) spectrum. Detailed numerical calculations of the keV-MeV spectrum of GRB photospheres [93, 24] show that a peak can appear at MeV and a non-thermal tail extends into the multi-MeV range. Then, upscattering of such photospheric photons by internal shock electrons [32] can lead to an up-scattered photospheric (UP) component of GeV photons (see Fig. 3, where  $k = U_{syn}/U_{up}$  is the ratio of synchrotron to upscattered photospheric emission by the internal shock, and  $x = L_{up}/L_{ph}$  is the ratio of upscattered photospheric to photospheric emission). This results in a broad-band spectrum similar to that seen by the *Fermi LAT /GBM* (e.g. Fig. 2). Time dependent numerical simulations of jets (e.g. [92]) indicate the possibility of photosphere and internal shock parameters leading to either an overlap of the photospheric and the UP component (appearing as a simple Band spectrum), or to a separate and bright UP component, corresponding to the second spectral component seen in a fraction of *LAT* GRBs [32].

Numerical calculations have been carried out [30] of the time-dependent spectral changes expected in generic dissipation regions (e.g., internal shocks, magnetic dissipation, etc.), incorporating all leptonic processes, have shown that one-zone models are inadequate to reproduce the observed GeV-MeV



delays. On the other hand, a multi-zone model injecting different spectral components at various initial injection times and angles into a geometrically and physically separate scattering zone [30] provides GeV-MeV time delays of the right magnitude. These could be, e.g. as above, a photosphere providing a Band spectrum plus a second dissipation zone further out which upscatters these photons.

## 5 Some Issues about Prompt Emission

The simple leptonic synchrotron (plus inverse Compton) interpretation of the non-thermal aspect of GRB radiation is the most straightforward, and is used in preference to others due to its simplicity. However, a number of effects can modify the simple synchrotron spectrum. One is that the cooling could be rapid, i.e. when the comoving synchrotron cooling time  $t'_{sy} = (9m_e^3 c^5 / 4e^4 B'^2 \gamma_e) \sim 7 \times 10^8 / B'^2 \gamma_e$  s is less than the comoving dynamic time  $t'_{dyn} \sim r / 2c\Gamma$ , the electrons cool down to  $\gamma_c = 6\pi m_e c / \sigma_T B'^2 t'_{dyn}$  and the spectrum above  $\nu_c \sim \Gamma(3/8\pi)(eB'/m_e c)\gamma_c^2$  is  $F_\nu \propto \nu^{-1/2}$  [61, 62]. Also, the distribution of observed low energy spectral indices  $\beta_1$  (where  $F_\nu \propto \nu^{\beta_1}$  below the spectral peak) has a mean value  $\beta_1 \sim 0$ , but for a fraction of bursts this slope reaches positive values  $\beta_1 > 1/3$  which are incompatible with a simple synchrotron interpretation [63]. Possible explanations include synchrotron self-absorption in the X-ray [64] or in the optical range up-scattered to X-rays [65], low-pitch angle scattering or jitter radiation [66, 67], observational selection biases [68] and/or time-dependent acceleration and radiation [69] where low-pitch angle diffusion can also explain high energy indices steeper than predicted by isotropic scattering. Other models invoke a photospheric component and pair formation [71], see below.

Other recent alternatives to the simple leptonic prompt emission mechanisms have continued to be motivated by concerns about the low radiative efficiency and fine-tuning needed to achieve the right peak energy and spectrum in an internal shock synchrotron interpretation. One proposal is based on a relativistic turbulence model [73, 72], which argues that relativistic eddies with Lorentz factors  $\gamma_r \sim 10$  in the comoving frame of the bulk  $\Gamma \gtrsim 300$  outflow survive to undergo at least  $\gamma_r$  changes over a dynamic time, leading both to high variability and better efficiency. Various constraints may however pose difficulties [74], while numerical simulations [46] indicate that relativistic turbulence would lead to shocks and thermalization, reducing it to

non-relativistic. A different dissipation model, entitled ICMART [47] involves a hybrid magnetically dominated outflow leading to semi-relativistic turbulent reconnection. Here a moderately magnetized  $\sigma = (B'^2/4\pi\rho'c^2) \lesssim 100$  MHD outflow undergoes internal shocks as  $\sigma \rightarrow 1$ , leading to turbulence and reconnection which accelerates electrons at radii  $r \gtrsim 10^{15}$  cm. These involve fewer protons than usual baryonic models, hence less conspicuous photospheres, and have significant variability, and the efficiency and spectrum are argued to have advantages over the usual synchrotron internal shocks (see also [37]. General issues of the acceleration of high- $\sigma$  relativistic flows were considered by [76], while more detailed models were discussed by [83, 77, 78].

## 6 Hadronic GRB Models

If GRB jets are baryon loaded, the charged baryons are likely to be co-accelerated in shocks, reconnection zones, etc., and hadronic processes would lead to both secondary high energy photons and neutrinos. Monte Carlo codes have been developed to model hadronic effects in relativistic flows, including  $p, \gamma$  cascades, Bethe-Heitler interactions, etc. E.g., one such code [29, 35] was used to calculate the photon spectra in GRBs from secondary leptons resulting from hadronic interactions following the acceleration of protons in the same shocks that accelerate primary electrons. The code uses an escape probability formulation to compute the emerging spectra in a steady state, and provides a detailed quantification of the signatures of hadronic interactions, which can be compared to those arising from purely leptonic acceleration. Spectral fits of the *Fermi LAT* observations of the short GRB 090510 were modeled by [54] as electron synchrotron for the MeV component and photohadronic cascade radiation for the GeV distinct power law component (Fig. 4).

Furthermore, since acceleration as well as cascade development can take additional time, even one-zone models might in principle lead to GeV-MeV delays, e.g. in a model [33] where the prompt MeV is electron synchrotron and the GeV is due to proton synchrotron, whose cooling time brings down the typical photon energy into the GeV on the delay timescale, and the electron plus proton synchrotron emission merge into a single Band function with an approximate spectral slope of the GeV photons.

Hadronic interactions can also have interesting implications for GRB optical prompt flashes. E.g., as discussed in [36], besides the usual Band MeV

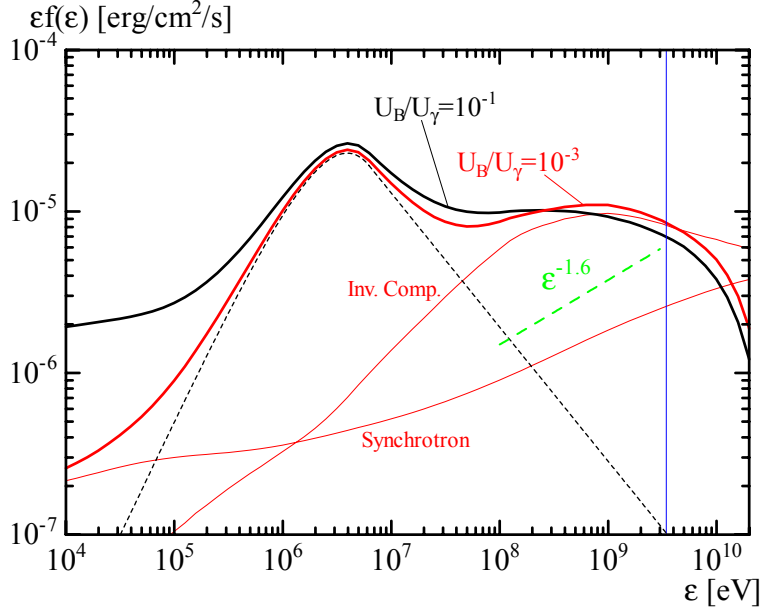


Figure 4:  $\nu F_\nu$  spectra (bold curve) from a hadronic model of GRB 090510. The red curve is for  $U_B/U_\gamma = 10^{-3}$  and  $L_p/L_\gamma = 200$ , and the black curve is for  $U_B/U_\gamma = 10^{-1}$  and  $L_p/L_\gamma = 30$ . Fine red curves denote separately pair synchrotron and inverse Compton from hadronic cascade secondaries, without absorption effects. The fine dashed curve is the Band component, the green dashed line is an approximate spectral slope of the GeV photons, the vertical blue line denotes the energy of the 3.4 GeV photon [54].

spectrum produced by conventional leptonic mechanisms, the acceleration of hadrons leads to secondaries whose radiation results not only in a high energy component but also in a prompt bright optical emission from secondary synchrotron. This could, in principle, explain the observed “naked eye” 5th magnitude flash of GRB 080319B, e.g. [94].

Hadronic binary collisions in baryon-loaded jets may also be important, both for producing efficient kinetic energy dissipation and for shaping the photon spectrum. This is because the baryons will consist (largely) of both protons ( $p$ ) and neutrons ( $n$ ), especially if heavy elements are photo-dissociated. The protons are coupled to the radiation during the acceleration phase but the neutrons are carried along only thanks to nuclear ( $p, n$ ) elastic collisions, whose characteristic timescale at some point becomes longer than the expan-

sion time. At this point the  $p$  and  $n$  relative drift velocity  $v$  approaches  $c$ , leading to the collisions becoming inelastic,  $p + n \rightarrow \pi^+, \pi^0$ , in turn leading to positrons, gamma-rays and neutrinos [95]. Such inelastic (p,n) collisions can also arise in jets where the bulk Lorentz factor is transversely inhomogeneous [70], e.g. going from large to small as the angle increases, as expected intuitively from a jet experiencing friction against the surrounding stellar envelope. In such cases, the neutrons from the slower, outer jet regions can diffuse into the faster inner regions, leading to inelastic (p,n) and (n,n) collisions resulting again in pions. An interesting consequence of either radial or tangential (n,p) drifts is that the decoupling generally occurs below the scattering photosphere, and the resulting positrons and gamma-rays deposit a significant fraction of the relative kinetic energy into the flow, reheating it [24]. Internal dissipation below the photosphere has been advocated, e.g. [42] to explain the MeV peaks as quasi-thermal photospheric peaks [22, 44], while having a large radiative efficiency. Such internal dissipation is naturally provided by (p,n) decoupling, and numerical simulations [24] indicate that a Band spectrum and a high efficiency is indeed obtained, which remains the case even when the flow is magnetized up to  $\varepsilon_B = 2$  [45], while keeping the dynamics dominated by the baryons. These numerical results were obtained for nominal cases based on a specific radial (n,p) velocity difference, although the phenomenon is generic.

## 7 Magnetic GRB Models

Magnetically dominated (or Poynting dominated) GRB jets fall into two categories, one where baryons are absent or dynamically negligible, at least initially, and another where the baryon load is significant although dynamically sub-dominant relative to the magnetic stresses.

The baryon-free Poynting jet models resemble pulsar wind models, except for being jet-shaped, as in AGN baryon-poor models. The energy requirements of GRB (isotropic-equivalent luminosities  $L_\gamma \gtrsim 10^{52}$  erg s $^{-1}$ ) require magnetic fields at the base in excess of  $B \sim 10^{15}$  G, which can be produced by shear and instabilities in an accreting torus around the BH. The energy source can be either the accretion energy, or via the magnetic coupling between the disk and BH, extraction of angular momentum from the latter occurring via the Blandford-Znajek mechanism [55]. The stresses in this type of model are initially magnetic, involving also pairs and photons, and

just as in purely hydro baryon-loaded models they lead to an initial Lorentz factor growth  $\Gamma \propto r$  up to a pair annihilation photosphere [39]. This provides a first radiation component, typically peaking in the hard X-ray to MeV, with upscattering adding a high energy power law. Internal shocks are not expected beyond this photosphere, but an external shock provides another IC component, which reaches into the GeV-TeV range. Such Poynting dominated models [48] may also be characteristic of Pop. III GRBs, whose X-ray and GeV spectra may be detectable [1]. Both the ‘prompt’ emission and the longer-lasting afterglows [84] of such Pop. III GRBs should be detectable with the BAT or XRT on *Swift* or the GBM on *Fermi*. On *Swift*, image triggers may be the best way to detect them, and some constraints on their rate are provided by radio surveys. They are expected to have GeV extensions as well, but redshift determinations need to rely on L-band or K-band spectroscopy.

The baryon-loaded magnetically dominated jets have a different acceleration dynamics than the baryon-poor magnetic jets or the baryon dominated hydrodynamic jets: whereas both the latter accelerate initially as  $\Gamma \propto r$  and eventually achieve a coasting Lorentz factor  $\Gamma_f \sim L_\gamma/Mc^2$ , the baryon-loaded magnetically dominated jets have a variety of possible acceleration behaviors, generally less steep than the above. In the simplest treatment of a homogeneous jet with transverse magnetic field which undergoes reconnection, the acceleration is  $\Gamma \propto r^{1/3}$  [56, 2], while in inhomogeneous jets where the magnetic field and the rest mass varies across the jet the average acceleration ranges from  $\Gamma \propto r^{1/3}$  to various other power laws intermediate between this and  $\Gamma \propto r$  [49, 96]. Few calculations have been made [97] of the expected (leptonic) spectral signatures in the simpler magnetized outflows, typically in a one-zone steady state approximation.

The photon spectral signatures of a magnetically dominated, baryon loaded leptonic + hadronic GRB model involving nuclear collisions has been calculated by [2]. This uses a realistic transverse structure of a fast core-slow sheath. The analytical results indicate that the transverse neutron collisions become most effective, resulting in GeV photons at radii from which the observer-frame time delay relative to the photospheric MeV photons is appropriate to explain the observed *Fermi* time lags. The purely leptonic (SSC, EIC) time delays and spectral components of such a baryon-loaded magnetic model, in the absence of drifts and transverse gradients, have been calculated by [7], leading to results in the range observed by *Fermi*.

## 8 High Redshift GRBs

GRBs are being identified at increasingly large redshifts, e.g. GRB080913 at  $z = 6.7$  [81], GRB090423 at  $z = 8.2$  [79, 80] (through spectroscopy), and GRB 090429B has been ascribed a photometric redshift of  $z \simeq 9.4$  [86]. It is possible that even more distant objects than these have already been detected in the gamma- and X-ray detectors of *Swift* and *Fermi*, although in the absence of a specific (optical/IR or other) redshift signature one cannot at present be sure of it, redshift diagnostics being increasingly harder to obtain in this range. The above discoveries do, however, indicate that the prospect of eventually reaching into the realm of Pop. III objects is becoming increasingly realistic. Pop. III GRBs may arise from very massive, metal-poor stars whose core collapses to a  $100 - 500M_{\odot}$  black hole [82]. The jets are likely to be Poynting-dominated, being powered by the Blandford-Znajek mechanism. The expansion dynamics and the radiation arising from such very massive Poynting jet GRBs was discussed by [1]. At typical redshifts  $z \sim 20$  this implies a “prompt” emission extending to  $\lesssim 1$  day which should be detectable by *Swift* or *Fermi*, being most prominent initially around 50 keV due to the jet pair photosphere, followed after a similar time interval by an external shock synchrotron component at a few keV and an inverse Compton component at  $\gtrsim 70$  GeV [32].

## 9 Non-photonic GRB Signals

The two main non-photonic signals that may be expected from GRBs are gravitational waves (GW) and high energy neutrinos (HENUs). The most likely GW emitters are short GRBs [112], if these indeed arise from merging compact objects [107]. The rates in advanced LIGO [53] and VIRGO may be at least several per year [113]. Long GRBs, more speculatively, might be detectable in GWs if they go through a magnetar phase [114], or if the core collapse breaks up into substantial blobs [115]; more detailed numerical calculations of collapsar (long) GRBs lead to GW prospects which range from pessimistic [116] to modest [117].

High energy neutrinos may be expected from baryon-loaded GRBs if sufficient protons are co-accelerated in the shocks. The most widely considered paradigm involves proton acceleration and  $p\gamma$  interactions in internal shocks, resulting in prompt  $\sim 100$  TeV HENUs [119, 120]. Other interaction re-

gions considered are external shocks, with  $p\gamma$  interactions on reverse shock UV photons leading to EeV HENUs [121]; and pre-emerging or choked jets in collapsars resulting in HENU precursors [122]. An EeV neutrino flux is also expected from external shocks in very massive Pop. III magnetically dominated GRBs [85]. Current IceCube observations [123, 124] are putting significant constraints on the internal shock neutrino emission model, with data from the full array still to be analyzed.

## 10 GRBs and CTA

Measurements by *LAT* have led to the conclusion that at least a fraction of GRB are emitting (in their own rest frame) photons in the energy range of at least up to 30 – 90 GeV. A list of Fermi *LAT* detections [101] of maximum observer-frame photon energies and corresponding redshifts ( $E_{\gamma,obs}, z$ ) is (13.2, 4.35), (7.5, 3.57), (5.3, 0.74), (31.3, 0.90), (33.4, 1.82), (19.6, 2.10), (2.8, 0.897), (4.3, 1.37). Two things emerge from this list: even  $z > 4$  bursts can produce  $E_{\gamma} > 10$  GeV photons at the observer, and some  $z \sim 1$  bursts can produce  $E_{\gamma} > 30$  GeV photons at the observer. This is highly encouraging for CTA, whether for a 'baseline' threshold of 25 GeV or for an 'optimistic' threshold of 10 GeV envisaged in recent CTA reviews [100]. The rate of detection by CTA is estimated by [100] to be 0.7 – 1.6 per year, based on the rate of Swift triggers (while GBM triggers on Fermi are more frequent, their positional accuracy is poorer). This estimated CTA rate is uncertain, since work continues on the evaluation of the actual fraction of bursts which emit in the GeV range, relative to those which are detected below 100 MeV [99, 98]. As of February 2011, in 2.5 years, Fermi *LAT* detected 4 bursts at energies  $> 10$  GeV (or 20 at  $> 0.1$  GeV) out of some 700 bursts detected by Fermi GBM at  $E < 100$  MeV. This very small fraction of the total ( $\lesssim 1\%$ ) of course is in part due to the size constraints under which space detectors must operate. The question is what is the real fraction of GRBs, whether long or short, which emits significantly at  $\gtrsim 10 - 20$  GeV.

In the usual internal shock model of prompt emission, the intra-source  $\gamma\gamma$  absorption typically prevents photons in excess of a few GeV to emerge [108, 109], unless the bulk Lorentz factor is above  $\sim 700$  [102]. For photospheric models of the prompt emission, e.g. [24], photons in excess of 10 GeV can escape the source from radii  $r_{\gamma\gamma} \sim 10^{15}$  cm, and such radii are also inferred phenomenologically from one-zone analyses of the Fermi data

on GRB. For the purposes of CTA, however, it is the afterglow, or extended, GeV emission that is of most interest. In the standard external shock scenario, the compactness parameter is smaller, and inverse Compton scattering is expected to lead to multi-GeV and TeV photons [40, 118], the details depending on the electron distribution slope and the radiative regime (e.g. slow or fast cooling). This scenario is thought to be responsible for the afterglows of GRB [38], and is also thought to be responsible for the extended GeV emission observed by LAT so far [26, 89, 91, 111], etc. Of course, propagation in the intergalactic medium from high redshifts leads to additional  $\gamma\gamma \rightarrow e^\pm$  interaction with the extragalactic background light, or EBL [103, 105, 104], the threshold for which depends on the photon energy and the source redshift.

Thus, while TeV emission, if produced, is mainly expected to be detectable from  $z \lesssim 0.5$ , the 10-30 GeV emission should be detectable from higher redshifts, as verified by the measurements mentioned above. Therefore, in the GeV range the detectability is dictated by the source physics, the source rate and the immediate source environment. The source rate, based on MeV observations, is well constrained [107], while the effects of the near-source environment can be reasonably parametrized (e.g. [106]). The source physics, however, offers larger uncertainties. This is because in an external shock model the simple synchrotron self-Compton (SSC) model can be additionally complicated by the scattering of photons arising at other locations, in particular well inside the external shock, e.g. from the jet photosphere [32], or from an inner region energized by continued central engine activity [110]. Similar uncertainties about the soft photon source and location would affect hadronic cascade models. Observationally, in some cases the GBM high energy spectral slopes are steep enough not to expect much GeV emission from their extrapolation [101], while in other cases the LAT spectrum shows a cutoff or turnover, e.g. in GRB 090926B [18]. Nonetheless, with all things considered, the estimate [100] of 0.7 – 1.6 CTA detections per year appears to be a conservative lower limit.

I am grateful to N. Omodei, S. Razzaque and P. Veres for valuable discussions. This research was supported in part by NASA NNX08AL40G and NSF PHY-0757155.

## References

- [1] Mészáros, P. and Rees, M.J., 2010, *ApJ*, 715:967
- [2] Mészáros, P. and Rees, M.J., 2011, *ApJ(Lett.)*, 733:L40



- [3] [Fermi Collaboration] Band, D. L. et al. 2009, *ApJ*, 701, 1673
- [4] Baring, M. G. 2006, *ApJ*, 650, 1004
- [5] Giuliani, A., et al. 2008, *A&A*, 491, L25
- [6] González, M. M., Dingus, B. L., Kaneko, Y., Preece, R. D., Dermer, C. D., & Briggs, M. S. 2003, *Nature*, 424, 749
- [7] Bosnjak, Z., Kumar, P., 2011, *MNRAS* subm., arXiv:1108.0929
- [8] Kaneko, Y., González, M. M., Preece, R. D., Dingus, B. L., & Briggs, M. S. 2008, *ApJ*, 677, 1168
- [9] Hurley, K, et al. 1994, *Nature*, 372, 652
- [10] Corsi, A. Guetta, D., Piro, L., 2010, *ApJ*, 720:1008
- [11] Abdo, A. A., et al. 2010, *ApJ*, 712, 558
- [12] [Fermi Collaboration] Ackermann, M., et al., 2010, *ApJ*, 716, 1178
- [13] De Pasquale, M., et al. 2010, *ApJL*, 709, L146
- [14] Razzaque, S. 2010, *ApJL*, 724, L109
- [15] [Fermi Collaboration] Abdo, A. A., et al. 2009, *Science*, 323, 1688
- [16] [Fermi Collaboration] Abdo, A. A., et al. 2009, *Nature*, 462, 331
- [17] [Fermi Collaboration] Abdo, A. A., et al. 2009, *ApJL*, 706, L138
- [18] [Fermi Collaboration] Ackermann, M., et al. 2011, *ApJ*, 729, 114
- [19] Guiriec, S., Briggs, M. S., Connaughton, V., et al. 2010, *ApJ*, 725, 225
- [20] Guiriec, S., Connaughton, V., Briggs, M. S., et al. 2011, *ApJL*, 727, L33
  
- [21] He, H-N., Wu, X-F., Toma, K., Wang, X-Y. and Mészáros, P., 2011, *ApJ*, 733:22
- [22] Ryde, F., Axelsson, M., Zhang, B. B., et al. 2010, *ApJL*, 709, L172
- [23] Granot, J., Cohen-Tanugi, J., & do Couto e Silva, E. 2008, *ApJ*, 677, 92
- [24] Beloborodov, A. M. 2010, *MNRAS*, 407, 1033
- [25] [Fermi Collaboration] Abdo, A. A., et al. 2010, *ApJ*, 723, 1082
- [26] Ghisellini, G., Ghirlanda, G., Nava, L., & Celotti, A. 2010, *MNRAS*, 403, 926
- [27] Li, Z. 2010, *ApJ*, 709, 525
- [28] Zou, Y.-C., Fan, Y.-Z., & Piran, T. 2011, *ApJL*, 726, L2
- [29] Asano, K., Inoue, S., & Mészáros, P., 2009a, *ApJ*, 699:953
- [30] Asano, K., & Mészáros, P. 2011, *ApJ*, in press (arXiv:1107.4825)
- [31] Toma, K., Wu, X., & Mészáros, P. 2009, *ApJ*, 707, 1404
- [32] Toma, K., Wu, X-F., & Mészáros, P. 2011, *MNRAS*, 415, 1663

- [33] Razzaque, S., Dermer, C., Fink, J. 2010, *The Open Astronomy Journal*, 3, 150 (arXiv:0908.0513)
- [34] Dermer, C. D., & Razzaque, S., 2010, *ApJ*, 724:1366
- [35] Asano, K., Guiriec, S., & Mészáros, P. 2009, *ApJL*, 705, L191
- [36] Asano, K., Inoue, S., & Mészáros, P. 2010, *ApJL*, 725, L121
- [37] Murase, K., Asano, K., Terasawa, T., & Mészáros, P., 2012, *ApJ*, 746:164
- [38] Mészáros, P. and Rees, M.J., 1997a, *ApJ*, 476:232
- [39] Mészáros, P. and Rees, M.J., 1997b, *ApJ*, 482:L29
- [40] Mészáros, P., Rees, M.J. and Papatthanassiou, H., 1994a, *ApJ*, 432:181
- [41] Mészáros, P. and Rees, M.J., 1994b, *MNRAS*, 269:L41
- [42] Rees, M.J. and Mészáros, P., 2005, *ApJ*, 628:847
- [43] Piran, T., & Nakar, E., 2010, *ApJ(Lett)* 718:L63
- [44] Pe'er, A., et al. 2012, *MNRAS* in press (arXiv:1007.2228)
- [45] Vurm, I., et al. 2011, *ApJ* 738:77
- [46] Zhang, W., & MacFadyen, A., 2009, *ApJ*, 698:1261
- [47] Zhang, B., & Yan, H. 2011, *ApJ*, 726, 90
- [48] Lyutikov, M., & Blandford, R. 2003 (arXiv:astro-ph/0312347)
- [49] McKinney, J., & Uzdensky, D. 2011, *MNRAS*, in press (arXiv:1011.1904)
- [50] [Fermi Collaboration] Abdo, A. A., et al. 2011, *ApJL*, 734:L27
- [51] <http://hawc.umd.edu/>
- [52] HAWC collaboration; Abeysekara, A. U., et al., 2011, (arXiv:1108.6034)
- [53] <https://www.advancedligo.mit.edu/>
- [54] Asano, K., Guiriec, S., & Mészáros, P., 2009b, *ApJ(Lett.)*, 705:L191
- [55] Blandford R.D. and Znajek R.L., 1977, *MNRAS*, 179:433
- [56] Drenkhahn, G. and Spruit, H.C., 2002, *A&A*, 391;1141
- [57] Giannios, D., Mimica, P. and Aloy, M. A., 2007, *A&A*, 478:747
- [58] Goldreich, P. and Julian, W.H., 1969, *ApJ* 157:869
- [59] Heger A., Woosley S.E., 2002, *ApJ*, 567:532
- [60] Heger, A, Fryer, CL, Woosley, SE, Langer, N and Hartmann, DH, 2003, *ApJ*, 591:288
- [61] Sari, R, Piran, T & Narayan, R, 1998, *ApJ*, 497, L17
- [62] Ghisellini, G. and Celotti, A. (1999), *ApJ*, 511, L93

- [63] Preece, R, Briggs M, Mallozzi R, Pendleton G, Paciesas W, Band D . 2000. ApJ(Sup.) 126:19
- [64] Granot J, Piran T, Sari R, 2000, ApJ, 534:L163
- [65] Panaitescu A & Mészáros P. 2000. ApJ 544:L17
- [66] Medvedev A. 2000. ApJ 540:704
- [67] Medvedev A, 2006, ApJ 637:869
- [68] Lloyd N & Petrosian V. 2001a. ApJ 543:722
- [69] Lloyd-Ronning, N & Petrosian, V, 2002, ApJ 543:722
- [70] Mészáros , P. and Rees, M.J., 2000a, Ap.J.(Lett.), 541:L5
- [71] Mészáros P & Rees MJ. 2000b, ApJ 530:292
- [72] Kumar, P., & Narayan, R., 2009, MNRAS 395:472
- [73] Narayan, R., & Kumar, P., 2009, MNRAS, 349:L117
- [74] Lazar, A., & Piran, T., 2009, ApJ, 695:L10
- [75] Zhang, W. Q., MacFadyen, A., & Wang, P., 2009, ApJ(Lett.), 692:L40
- [76] Lyutikov, M., 2010, arXiv:1004.2429
- [77] Granot, J., et al, 2010, arXiv:1004.0959
- [78] Granot, J., 2011b, arXiv:1109.5315
- [79] Tanvir, N., et al, 2009, Nature, 461:1254
- [80] Salvaterra, R., et al., 2009, Nature, 461:1258
- [81] Greiner, J., et al, 2009, ApJ, 693:1610
- [82] Komissarov, S., & Barkov, M., 2010, MNRAS, 402:L25
- [83] Komissarov, S., Vlahakis, N. & Koenigl, A., 2010b, MNRAS, 407:17
- [84] Toma, K., Sakamoto, T. and Mészáros , P., 2011, ApJ, 731:127
- [85] Gao, S., Toma, K. and Mészáros , P., Phys.Rev. D, 83:103004
- [86] Cucchiara, A, et al, 2011, ApJ, 736:7
- [87] Kumar, P., & Barniol Duran, R. 2009, MNRAS, 400, L75
- [88] Kumar, P., & Barniol-Duran, R., 2010a, arXiv:0905.2417
- [89] Kumar, P., & Barniol-Duran, R., 2010b, MNRAS, 409:226
- [90] Kumar, P., & Barniol-Duran, R., 2010c, arXiv:1003.5916
- [91] Wang, X. Y., et al, 2010, ApJ, 712: 1232
- [92] Lazzati, D., et al, 2009, ApJ, 700:L47
- [93] Lazzati, D., & Begelman, M., 2010, arXiv:1005.4704
- [94] Racusin, J., et al., 2008, Nature, 455:183
- [95] Bahcall, J. N. and Mészáros , P., 2000, Phys. Rev. Lett., 85:1362

- [96] Metzger, B.D., Giannios, D., Thompson, T.A., Bucciantini, N. and Quataert, E., 2011, M.N.R.A.S. in press (arXiv:1012.0001)
- [97] Giannios, D. and Spruit, H.C., 2007, A&A 469:L1
- [98] Beniamini, P., et al., 2011, MNRAS, 416:3089
- [99] Guetta, D., Pian, E. and Waxman, E., 2011, A& A, 525:A53
- [100] Bouvier, A., et al., 2011, Procs. 32nd ICRC, Beijing; arXiv:1109.5680
- [101] Omodei, N., et al., 2011, talk at Fermi Symposium, Feb. 2011; 1st Fermi GRB catalog, in prep.
- [102] Razzaque, S., Mészáros, P. and Zhang, B., 2004, ApJ, 613:1072
- [103] Coppi, P. and Aharonian, F., 1997, ApJ(Lett.), 487:L9
- [104] Primack, J., et al., 2011, AIPC, 1381:72
- [105] Finke, J., Razzaque, S. and Dermer, C., 2010, ApJ, 712:238
- [106] Gilmore, R. and Ramirez-Ruiz, E., 2010, ApJ, 721:709
- [107] Gehrels, N., Ramirez-Ruiz, E. and Fox, D., ARAA, 47:567
- [108] Papathanassiou, H. and Mészáros, P., 1996, ApJ(Lett.), 471:L91
- [109] Pilla, R. P. and Loeb, A., 1998, ApJ(Lett.), 494:L167
- [110] Wang, X.-Y., Li, Z. and Mészáros, P., 2006, ApJ(Lett), 641:L89
- [111] Zhang, B-B., et al, 2011, ApJ, 730:141
- [112] Centrella, J., 2011, AIPC, 1381:98
- [113] Leonor, I. et al, 2009, Class. Qu. Grav., 26:20
- [114] Corsi, A. and Mészáros, P., 2009, Ap.J., 702:1171
- [115] Kobayashi, S. and Mészáros, P., 2003, ApJ, 589:861
- [116] Ott, C.D., et al, 2011, Phys.Rev.Lett.. 106:161103
- [117] Kiuchi, K. et al, 2011, Phys.Rev.Lett., 106:251102
- [118] Mészáros, P. and Rees, M.J., 1994, M.N.R.A.S., 269:L41
- [119] Waxman, E. and Bahcall, J.N., 1997, Phys.rev.Lett. 78:2291
- [120] Murase, K. and Nagataki, S., 2006, Phys.Rev.D, 73:063002
- [121] Waxman, E. and Bahcall, J.N., 2000, ApJ, 541:707
- [122] Mészáros, P. and Waxman, E., 2001, Phys.Rev.Lett., 2001, 87:171102
  
- [123] Ahlers, M. et al, 2011, ApPh, 35:87
- [124] Abbasi, R, et al, 2011, Phys.Rev,Lett. 106:141101